

Adiabatic Quantum Computing in systems with constant inter-qubit couplings

S. Knysch¹, V.N. Smelyanskiy²

¹Mission Critical Technologies, Inc., 2041 Rosecrans Avenue, Suite 225, El Segundo, CA 90245 and

²NASA Ames Research Center, Mail Stop 269-2, Moffett Field, CA 94035, USA

We propose an approach suitable for solving NP-complete problems via adiabatic quantum computation with an architecture based on a lattice of interacting spins (qubits) driven by locally adjustable effective magnetic fields. Interactions between qubits are assumed constant and instance-independent, programming is done only by changing local magnetic fields. Implementations using qubits coupled by magnetic-, electric-dipole and exchange interactions are discussed.

I. INTRODUCTION

It is one of the central open questions in the field of quantum computing if quantum algorithms can efficiently solve computationally hard problems in combinatorial optimization. The most common problems of this kind encountered in practice belong to a so-called NP-complete class [1] and are in almost one-to-one correspondence with the spin glass models in physics [2]. A basic property of these models is an onset of an exponentially large number of deep local minima of the energy landscape formed by spin configurations separated by a large number of spin flips.

A general framework for solving optimization problems on a quantum computer is provided by an Adiabatic Quantum Computation (AQC) [3, 4]. In its simplest form AQC corresponds to a "quantum annealing" (QA) of a spin system in the uniform transverse magnetic field described by a smoothly-varying in time Hamiltonian \hat{H}

$$\hat{H}(\Gamma) = -\Gamma \sum_{i=1}^N \hat{\sigma}_i^x + \hat{H}_0, \quad \Gamma \equiv \Gamma(t). \quad (1)$$

Γ is proportional to the transverse field strength; $\hat{\sigma}_i^x$ is a Pauli matrix for the i^{th} spin. The first term in (1) is called a "driver", it causes transitions between the eigenstates of the problem Hamiltonian \hat{H}_0 whose ground state encodes the solution of the classical optimization problem in question. For example, to find the ground state of the classical Ising model one uses

$$\hat{H}_0 = -\sum_{i=1}^N h_i \hat{\sigma}_z^i - \sum_{\langle i,k \rangle} J_{ik} \hat{\sigma}_i^z \hat{\sigma}_k^z, \quad (2)$$

where h_i are longitudinal fields acting on spins and the summation is over the pairs $\langle i, k \rangle$ of coupled lattice sites. In QA the value of $\Gamma = \Gamma(t) > 0$ is slowly decreasing in time from a large value $\Gamma_0 \gg \max(|J_{ij}|)$ at the start, to $\Gamma = 0$ at the end of the algorithm. The initial state is prepared to be a ground state of $H(\Gamma_0) \approx -\Gamma_0 \sum_{j=1}^N \hat{\sigma}_j^x$ with each spin pointing in the positive x-direction. For adiabatically slow variation of $\Gamma(t)$ the system state will be closely tracking the instantaneous ground state $|\psi_0(\Gamma)\rangle$ of $\hat{H}(\Gamma)$. It will approach the ground state of H_0 at the

end of the algorithm and the solution of the optimization problem can be recovered by measurements.

A metric for the performance of the AQC can be given in terms of the minimum value $g_{\min} = \min_{\Gamma} g(\Gamma)$ of the excitation gap $g(\Gamma)$ between the ground and first excited energy levels of $H(\Gamma)$. In particular, if $1/g_{\min}$ grows no faster than polynomially in the problem size N then so does the runtime of AQC.

It was demonstrated recently for AQC applied to computationally hard random instances of NP-complete Satisfiability problem that the algorithm performance is substantially affected by the existence of the first-order quantum phase transition for some value of $\Gamma = \Gamma^*$ in the limit $N \rightarrow \infty$ [5]. In this limit the instantaneous gap averaged over the ensemble of random problem instances vanishes, $\langle g(\Gamma^*) \rangle \rightarrow 0$. This produces a significant difficulty in the analysis of the asymptotic complexity of AQC. Indeed, assume that for a given problem instance \mathcal{I}_N of a finite size N the minimum gap is achieved at some value of $\Gamma = \Gamma_{\mathcal{I}_N}$. For large N the distribution of the values of $\Gamma_{\mathcal{I}_N}$ over the ensemble of random problem instances \mathcal{I}_N is peaked around Γ_* and has a width $\sim N^{-1/2}$. Therefore the minimum of the ensemble-averaged excitation gap, $\min_{\Gamma} \langle g \rangle$, will scale down polynomially with N . At the same time the ensemble average of the minimum gap $\langle \min_{\Gamma} g(\Gamma) \rangle$ can be exponentially small in N .

The above discussion implies that, in general, the order of time-minimization (over Γ) and statistical averaging of the excitation gap over the ensemble of problem instances *cannot* be inverted. Therefore static properties of the quantum phase transition (e.g., a phase diagram) are not sufficient to obtain the true asymptotic complexity of AQC and a daunting theoretical task of studying the *dynamics* of the phase transition is required. An crucial insight here can be gained from the experiments implementing AQC for problem instances of a large size.

An early work on this subject is a quantum annealing experiment [6]. It uses the macroscopic samples of a disordered magnet $\text{LiHo}_x\text{Y}_{1-x}\text{F}_4$ with the dipolar coupling between the spins that are formed by the doublet states of Ho^{+3} ions randomly substituted for nonmagnetic Y^{3+} . When the magnetic field is applied perpendicular to the Ising axes the system can be approximated by the Hamiltonian H (1),(2) corresponding to a quantum 3D Ising model with the random antiferromagnetic interaction between neighboring spins in the transverse

magnetic field $\Gamma = \Gamma(t)$.

For $\Gamma = 0$ finding a ground state of H can be mapped onto an NP-complete problem [7]. However this mapping is only approximate for the random magnet [6] because it is not exactly of the Ising type due to the very small components of the g-factor transverse to the Ising axis. Also the analog computation via QA [6] is of a low-fidelity type because it does not have any explicit control nor correction of the decoherence-induced errors, unlike the conventional quantum computation schemes based on quantum circuits. Finally, the adiabatic evolution in QA [6] collapses beyond the point $\Gamma_* > 0$ of a quantum phase transition from a quantum paramagnet to a quantum spin glass where the system escapes from the adiabatic ground state to states with low-lying energy levels forming a quasi-continuous spectrum [8].

Despite all these shortcomings the magnetic susceptibility study in [6] and the subsequent numerical simulations of this system [8] shows that QA provides a dramatic speedup of convergence to low-energy states of $\text{LiHo}_x\text{Y}_{1-x}\text{F}_4$ over a purely thermal annealing procedure at zero transverse magnetic field. This was attributed to the fact that the tunnelling processes between local minima of the energy landscape open up new transition pathways as compared to thermally activated spin flips.

The decoherence rate for the lowest doublet (spin) states in Ho ions comes from the coupling to Ho nuclei and is small [9],[10](a), possibly much smaller than the level splitting and magnetic dipolar coupling between the neighboring Ho spins [11]. One can expect that the success of QA is based substantially on a strong build-in quantum coherence with extremely entangled many-spin states and quantum correlations extending out over large group of spins (cf. [10](b)).

All NP-complete problems can be mapped onto one another by a classical algorithms that scale polynomially in the problem size N [1]. However different problems correspond to spin Hamiltonians with quite different physical properties, such as long-range *vs* short-range interactions, fully-connected *vs* sparsely-connected graphs, etc. Therefore it would be of a fundamental importance to experimentally study the properties of QA in mesoscopic systems modelling different NP-complete problems at $\Gamma = 0$. This can shed a light on the power of QA even if the experiments are of a low-fidelity type [6]. However one has to overcome several obstacles to implement this approach:

- (i) many NP-complete problems correspond to a long-range interaction between classical spins while the underlying physical systems have short-range interactions;
- (ii) in most of the perspective material systems the coupling between qubits is either difficult or impossible to control. The former includes systems with superconducting qubits [12, 13, 14, 15, 16] and the latter includes systems with magneto-dipole [23, 24, 25], electro-dipole [17, 18, 19, 20], and elastic-dipole

[21, 22] interactions;

- (iii) irregularities of the crystal lattice and random spatial positions of qubits give rise to the fluctuations in magnitude and sign of the qubit coupling coefficients across the sample.

Kaminsky, Lloyd and Orlando (KLO) [26] proposed a novel AQC architecture for solving NP-complete Maximum Independent Set problem using superconducting qubits. In their method an instance of the problem is converted into an equivalent circuit with ferromagnetic and antiferromagnetic couplings in a uniform magnetic field. In [26] switchable interqubit couplings using one of the mechanisms presented in [13, 28] are necessary for encoding an instance of MIS, but the architecture does not require a change in couplings during the algorithm execution for a given problem instance.

At the same time the couplings in [26] have to be readjusted for solving a new instance of MIS problem. Also the scalability of this is limited because it only allows the switching between the regimes of small and large couplings. I.e., it cannot guarantee that two sites are completely decoupled, nor the sign of the coupling can be changed.

In what following we propose the architecture for AQC that assumes that qubit couplings are *not* adjustable and addresses all the problems (i)-(iii) mentioned above. Moreover the architecture that we propose for solving various NP-complete problems via AQC is universal, in a sense that it is independent on any particular qubit implementation.

II. MAXIMUM INDEPENDENT SET PROBLEM

For practical implementation of AQC for solving an optimization problem it is necessary to translate this problem into a model Hamiltonian with single-spin and pairwise interactions only. It is especially straightforward to do for the NP-complete graph theory problem Maximum Independent Set (MIS) [26]. This problem is defined on a graph $G = (V, E)$ that is composed of the set of vertices V connected by edges from the set E . MIS is the problem of finding the largest subset S of vertices V such that no two vertices on the subset share an edge from E . The reason why this problem is well suited for AQC is that its solution is isomorphic to finding a ground state of an antiferromagnetically coupled Ising spin model in a uniform magnetic field [7].

The next obstacle has to do with the fact that we want to use spins on a 2D lattice and use only nearest-neighbor interactions. If the graph is non-planar it cannot be embedded into 2D lattice with nearest-neighbor interactions only. And there is no guarantee that a graph just constructed has a drawing on a plane without intersecting edges. Fortunately using a construction invented by Garey, Johnson and Stockmeyer [27] we can replace two intersecting edges by a gadget of Fig. 1. Maximizing

the independent set in the gadget reveals opposite vertices cannot both be occupied without incurring energy penalty. Solving MIS problem for the transformed graph gives the solution for the original one. Replacing all instances of intersecting edges by such gadget renders the graph planar. For this reason, without losing generality, we can restrict our discussion to planar graphs.

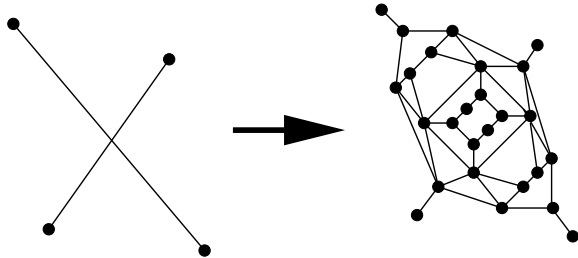


FIG. 1: Every intersection of two edges is replaced by a planar graph (right).

Before we describe the embedding of planar graph into a regular 2D lattice let us demonstrate how the MIS problem maps onto Ising model. We model vertices of the graph with classical Ising spins that can take values $s_i = \pm 1$. The edges correspond to antiferromagnetic interactions between spins. Consider the following classical Hamiltonian:

$$H_0 = - \sum_{\langle i,k \rangle} J_{i,k} s_i s_k + \sum_i s_i \sum_k J_{i,k} \quad (3)$$

where $J_{i,k} < 0$ corresponding to antiferromagnetic interaction and local magnetic fields are $h_i = \sum_k J_{i,k}$ (the sum is over the neighbors of a vertex i). This expression can be (up to a constant) rewritten as

$$H_0 = - \sum_{\langle i,k \rangle} J_{i,k} (1 - s_i)(1 - s_k). \quad (4)$$

Since all interactions are antiferromagnetic ($J_{i,k} < 0$) and $(1 - s_i)(1 - s_k) \geq 0$, we must have $H_0 \geq 0$. The minimum value $H_0 = 0$ is reached only if no edge $\langle i, k \rangle$ has both $s_i = -1$ and $s_k = -1$. In other words the set of vertices $\{i | s_i = -1\}$ is independent, no two vertices from this set share a vertex. Hence, the minima of H_0 are all possible independent sets. Next, we adjust individual magnetic fields $h'_i = h_i - J$, which is equivalent to adding a perturbation

$$V = J \sum_i s_i. \quad (5)$$

Its role is to maximize the number of vertices with $s_i = -1$, i.e. maximize the cardinality of MIS. By choosing $J \leq \min_{\langle i,k \rangle} |J_{i,k}|$ we guarantee that all minima of $H_0 + V$ correspond to independent sets with $H_0 = 0$. Indeed, if for some minimum of $H_0 + V$ and for some i, k both $s_i = -1$ and $s_k = -1$, then setting $s_i = +1$ decreases H_0 by at least $4|J_{i,k}| \geq 4J$ and at the same time increases V by $2J$.

The overall energy decreases by at least $2J$ contradicting our assumption that we started from a minimum of $H_0 + V$. Therefore, the ground states of $H_0 + V$ correspond to solutions of MIS problem. Moreover, the gap between ground state(s) and first excited state(s) is at least $2J$.

Obviously, very few planar graphs can be drawn on a lattice, with vertices corresponding to the nodes of the lattice and edges corresponding to nearest-neighbor links. In general case vertices have to be represented by whole clusters of spins. We generalize Hamiltonian (3) as follows. We label spins by two indices; in addition to cluster index i , we have index within a cluster α : $s_{i\alpha}$. Similarly, interactions are denoted by $J_{i\alpha, k\beta}$ which can be either ferromagnetic or antiferromagnetic. Restrictions on signs of interactions will be explained later, while as before we require $|J_{i\alpha, k\beta}| \geq J$. Within each cluster, the graph of interactions is a connected tree. Between clusters there is at most one link, and the link between clusters i and k is present if and only if there is an edge joining vertices i and k . This construction is illustrated in Fig. 2 for a simple graph.

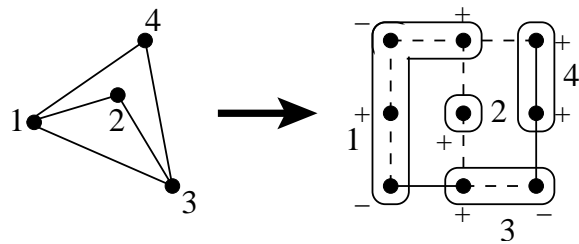


FIG. 2: An example graph with 4 vertices (left) is mapped onto another graph with vertices lying on the grid (right). Each vertex is replaced by clusters on the right. “+” and “-” signify values of corresponding $\tau_{i\alpha}$; solid and dashed lines represent ferromagnetic and antiferromagnetic interactions respectively.

The fact that the graph of interactions within a cluster is a tree means that when considered separately, each cluster has a doubly degenerate ground state. We identify them with values of fictitious coarse-grained spin S_i . Value $S_i = -1$ shall indicate that vertex i is included in the independent set. The individual spins take values $s_i = \tau_i S_i$ for appropriate τ_i . Clearly

$$J_{i\alpha, i\beta} \tau_{i\alpha} \tau_{i\beta} > 0. \quad (6)$$

In principle, values of $\tau_{i\alpha}$ can be deduced from $J_{i\alpha, i\beta}$ via the last equation, but in practice this will not be necessary since their values will be evident from the construction.

Between different clusters an interaction must be effectively antiferromagnetic. If there is a link between $s_{i\alpha}$ and $s_{k\beta}$, we require that

$$J_{i\alpha, k\beta} \tau_{i\alpha} \tau_{k\beta} < 0, \quad (7)$$

so that S_i and S_k are coupled antiferromagnetically.

Consider the Hamiltonian

$$H_0 = - \sum_i \sum_{\langle i\alpha, i\beta \rangle} J_{i\alpha, i\beta} s_{i\alpha} s_{i\beta} - \sum_{\langle i\alpha, k\beta \rangle} J_{i\alpha, k\beta} s_{i\alpha} s_{k\beta} - \sum_{i\alpha} h_{i\alpha} s_{i\alpha}. \quad (8)$$

Here in the first term the double summation is over the clusters i and over all edges $\langle i\alpha, i\beta \rangle$ within each cluster. In the second term the summation is over all pairs of distinct clusters $i \neq k$ connected by an edge $\langle i\alpha, k\beta \rangle$. Individual fields $h_{i\alpha}$ in (8) can be adjusted so that H_0 is rewritten (up to a constant) as $H_0 = H_1 + H_2$ with

$$H_1 = \sum_i \sum_{\langle i\alpha, i\beta \rangle} |J_{i\alpha, i\beta}| (1 - \tau_{i\alpha} \tau_{i\beta} s_{i\alpha} s_{i\beta}), \quad (9)$$

$$H_2 = \sum_{\langle i\alpha, k\beta \rangle} |J_{i\alpha, k\beta}| (1 - \tau_{i\alpha} s_{i\alpha}) (1 - \tau_{k\beta} s_{k\beta}). \quad (10)$$

(it can be verified that all signs above are correct given the inequalities (6) and (7)). In the above equations both $H_1 \geq 0$ and $H_2 \geq 0$. The ground state of H_0 corresponds to $H_1 = 0$ and $H_2 = 0$. The first equality $H_1 = 0$ implies $\tau_{i\alpha} s_{i\alpha} = \tau_{i\beta} s_{i\beta}$ for all α, β or, equivalently, $s_{i\alpha} = \tau_{i\alpha} S_i$ for all α . With this constraint in mind, H_2 can be rewritten into a familiar form $\sum_{\langle i\alpha, k\beta \rangle} |J_{i\alpha, k\beta}| (1 - S_i)(1 - S_k)$. Then $H_2 = 0$ implies that no two vertices i, k that are joined by an edge belong to the independent set at the same time ($S_i = S_k = -1$ is forbidden).

We now estimate the gap between ground states and excited states. If $H_1 \neq 0$ it must be at least $2|J_{i\alpha, i\beta}|$; and if $H_2 \neq 0$ it is at least $4|J_{i\alpha, k\beta}|$. Therefore the gap is at least $2J$. The degenerate ground states of H_0 correspond to all possible independent sets. This degeneracy is (partially) lifted by adding a term to H_0

$$H_0 = H_1 + H_2 + V, \quad V = \frac{J}{2} \sum_i s_{i0} \tau_{i0}, \quad (11)$$

where 0 is some arbitrary index within a cluster. This corresponds to adjusting $h'_{i0} = h_{i0} - \frac{J}{2} \tau_{i0}$. Alternatively, rather than pick up a particular spin $i\alpha$ we can adjust $h'_{i\alpha} = h_{i\alpha} - \frac{J}{2n_i} \tau_{i\alpha}$, where n_i is the size of cluster i . Then

$$V = \frac{J}{2} \sum_{i\alpha} \frac{s_{i\alpha} \tau_{i\alpha}}{n_i}. \quad (12)$$

In either case, the net effect is that the extra term takes a form $\frac{J}{2} \sum_i S_i$, which favors independent sets with the largest cardinality (number of vertices with $S_i = -1$ is maximized). We need only to verify that the perturbation V is small enough to not mix the ground states and excited states of H_0 . If either H_1 or H_2 is positive, then, for all spins within the corresponding cluster i we set $s_{i\alpha} = \tau_{i\alpha}$ (this is equivalent to setting $S_i = +1$). This decreases the energy by at least $2J$ as we have already estimated. On the other hand, the energy increase due

to degeneracy-breaking term is at most J . We conclude that the minima of H_0 involve only independent sets, and that the energy gap is at least J .

Once we have constructed a classical Hamiltonian H_0 (9)-(12) the ground state of which corresponds to the solution of NP-complete MIS problem, we formulate a quantum Hamiltonian \hat{H} (1) for use in the AQC by replacing in H_0 all classical spins $s_{i\alpha}$ with operators $\hat{\sigma}_{i\alpha}^z$ (cf. (2)) and adding a driver term $-\Gamma \sum_{i=1}^N \hat{\sigma}_i^x$.

III. EMBEDDING PLANAR GRAPH IN A LATTICE

As explained in the previous section, only planar graphs have to be considered. Also note that only connected graphs can be considered; for disconnected graphs we may solve the problem for each connected component. Every vertex of the planar graph is mapped onto a cluster of vertices and edges forming a tree. This allows vertices far from each other to be joined. Also we must always preserve an antiferromagnetic character of interactions between the vertices to satisfy the inequality (7).

An arbitrary planar graph can be mapped onto an appropriately sized regular lattice of spins with nearest neighbor interactions, as long as such system has a frustration (loops with odd number of antiferromagnetic couplings must exist). This is a necessary condition since the ground state of a non-frustrated system is trivially obtained, whereas a ground state of NP-complete problems typically has an exponentially large degeneracy, with degenerate states unrelated to each other by symmetry transformations.

For illustrative purposes we now embed a graph in a triangular lattice with antiferromagnetic interactions (so that each plaquette is frustrated), but such that every antiferromagnetic coupling can be switched off by an external control. A straightforward construction of a graph embedding is via iterated procedure. Let's label the vertices with numbers $1 \dots N$ subject to following constraints: a) vertex i is necessarily adjacent to at least one vertex j such that $j < i$, and b) if a set of vertices j_1, j_2, \dots, j_n, i forms a face of the planar graph and all $j_k < i$, all vertices that appear *inside* that face must have numbers smaller than i . Once we constructed an embedding of subgraph H of graph G , we augment H with a new vertex i connected to it. We extend the clusters corresponding to the vertices adjacent to i and link them to i . A completely blind procedure may not always work. Let us call the vertices from H "eligible" if they are adjacent to the vertices from G that do not belong to H ($G \setminus H$). Links from eligible vertices to some new vertex will have to be drawn at later stages.

In the case of a non-convex embedding of a subgraph H we may encounter a situation where there are not enough qubits in 2D lattice to draw all links from the new vertex to eligible vertices (see Fig.3). We can guarantee that this never happens if we use the following guidelines: we

always expand clusters corresponding to eligible vertices so that the embedding remains convex, eligible vertices lie on the perimeter of this convex region, and a minimum distance between eligible vertices along the perimeter is maintained. For the triangular lattice we make sure that

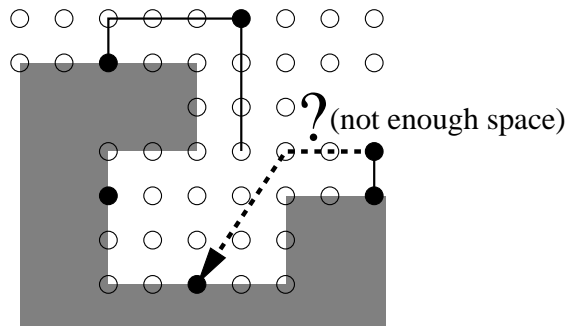


FIG. 3: An example of the case where a graph’s embedding has a non-convex shape and some eligible vertices (black circles) lie inside of the cavities. In this case there may not be enough space to connect all eligible vertices to outlying vertices. A gray area represents a part of the graph that is already embedded.

the convex object always has the form of a triangle. The distance between the eligible vertices along the perimeter must be at least two. Adding a vertex that is joined to subgraph H by only one edge increases the side of the triangle by 1 (see Fig. 4), and adding a vertex joined by two or more edges to subgraph H can increase the side of the triangle by 2 for the worst-case scenario depicted in Fig. 5.

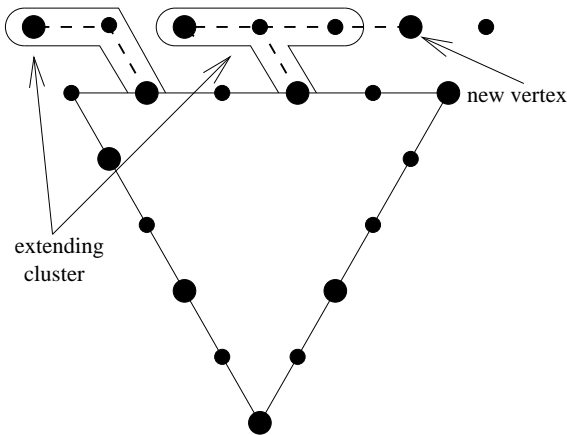


FIG. 4: All vertices on the top side are coupled ferromagnetically to the new side. A new vertex is introduced that is coupled antiferromagnetically [29].

We now explain Figs. 4 and 5 in more details. Large black circles lying on a boundary of the triangle describe the eligible vertices; connections to them may have to be made at a later stage. In Fig. 4 one vertex is added joined to the current subgraphs by one edge. It must be coupled antiferromagnetically to a cluster corresponding

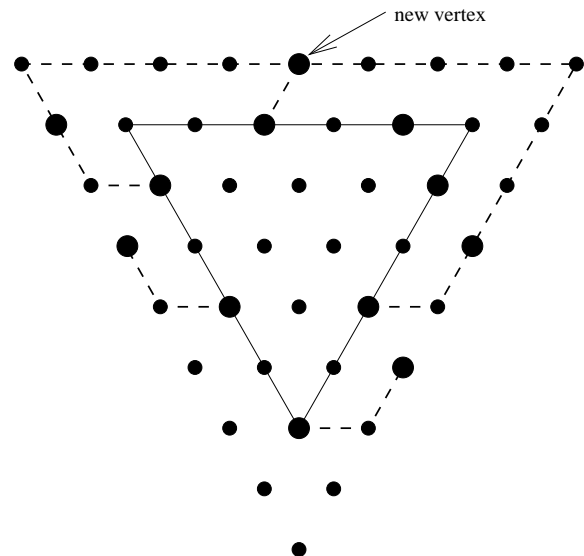


FIG. 5: A new vertex is connected via antiferromagnetic links. All other vertices coupled ferromagnetically to new sides [29].

to neighboring vertex [29].

A “copy” of the neighboring vertex is made since more vertices may connect to it later on. The cluster associated with that vertex is expanded to include that copy. Similarly, copies of all eligible vertices on the same side of the triangles are added to corresponding clusters. Note that copies of vertices are coupled ferromagnetically, whereas new vertex is coupled antiferromagnetically. This guarantees that for all large black circles the corresponding values of $\tau_{i\alpha} = 1$ and the inequalities (6),(7) are satisfied. In Fig. 5 a new vertex is connected to 3 vertices of the subgraph H . Copies of left and right vertices are made by ferromagnetic couplings. No copy of the middle vertex is made – it cannot be connected to new vertices as long as we add vertices in correct order. Fortunately, under the iteration in both cases a minimum distance of 2 between eligible vertices is maintained.

Let us now make some estimates. For a connected planar graph with N vertices and M edges the following inequality holds:

$$N - 1 \leq M \leq 3(N - 2). \quad (13)$$

Due to this tight bound, N alone is a good measure of the size of a graph. Let us now estimate the number of qubits needed in our construction. Adding each consecutive vertex may increase the side of the triangle by 2. A single vertex is represented by a single qubit. A triangle of size $2(N - 1)$ has $N(2N - 1) < 2N^2$ qubits. This presents an upper bound on the number of qubits needed to model a planar graph with N vertices. Note that we have used qubits quite liberally. We hope that far smaller number of qubits may be required for practical implementation, possibly a number scaling linearly with N . Minimization of this number is an interesting topic for further study.

IV. ADJUSTABLE COUPLINGS VS. FIXED COUPLINGS

The construction that we provided requires the programmability of nearest-neighbor interactions (i.e., the ability to switch them off). Embedding of NP-complete problems can only be done into the lattices that possess frustration. An antiferromagnet on a triangular lattice is always frustrated and therefore only the ability to switch off antiferromagnetic interactions is necessary in this case. However for a square lattice, switching between ferromagnetic, antiferromagnetic and zero couplings is necessary. This is because for a square lattice neither ferromagnet nor antiferromagnet has a frustration that requires the presence of interactions of both signs.

Antiferromagnetic triangular lattice with adjustable interactions can be implemented in superconducting QC by one of devices described in [13] and [28]. The idea to use them for implementing AQC was first put forward by Kaminsky, Lloyd and Orlando [26]. However the approach described in [26] cannot be used when switching between 3 states (ferromagnetic, antiferromagnetic and zero coupling) is needed. Moreover, the switching is not precisely between antiferromagnetic and zero couplings but rather between strong antiferromagnetic and weak antiferromagnetic couplings. While this is adequate for small graphs, for graphs that are sufficiently large ($O(J_{\text{on}}/J_{\text{off}})$), presence of weak antiferromagnetic coupling can lead to appearance of spurious minima unrelated to the correct solution of MIS problem. This effect can be compensated by grouping vertices in larger clusters and grouping links between qubits in these clusters in larger bundles. This approach is analogous to using thick “wires”, which increases $J_{\text{on}}/J_{\text{off}}$ ratio for effective interactions. This approach, however, is riddled with complexities. And most importantly, as was argued in Introduction, in many physical systems it is crucial to have an AQC architecture that does not rely *at all* on tunable interactions. This is precisely what we propose to accomplish in this paper.

A. Fixed interactions

The general idea of our approach is the following. Instead of “deleting” couplings between nodes of the regular lattice we propose to delete vertices. By applying a large (effective) magnetic field to a particular qubit i we can polarize it along the z direction (to value $+1$). Magnetic fields for its neighbors are adjusted as follows

$$h'_k = h_k - J_{i,k}. \quad (14)$$

The net effect is the same as if qubit i was completely absent (not coupled to its neighbors). Since this operation can be applied to any qubit, we can start from a regular lattice and by selecting a set of qubits to be deleted appropriately, we “carve out” a desired circuit. Note that, although we so far assumed that spins at deleted vertices

are completely polarized, corresponding to infinitely large magnetic fields, in practice we only require that spins be completely polarized in the ground state of the classical Hamiltonian. For that purpose it is sufficient to use magnetic fields on the order of J , defined as $J = \min_{(i,k)} J_{i,k}$.

We identify several solutions for implementing this. First general approach is to use one lattice where individual nodes are “deleted” to simulate another lattice with switchable interactions. The simulated lattice will have a larger lattice constant. Therefore a larger number of qubits is required. As a first example of this approach we take a square lattice with a particular periodic structure as depicted in Fig. 6. In this figure solid lines correspond to ferromagnetic and dashed line to antiferromagnetic couplings.

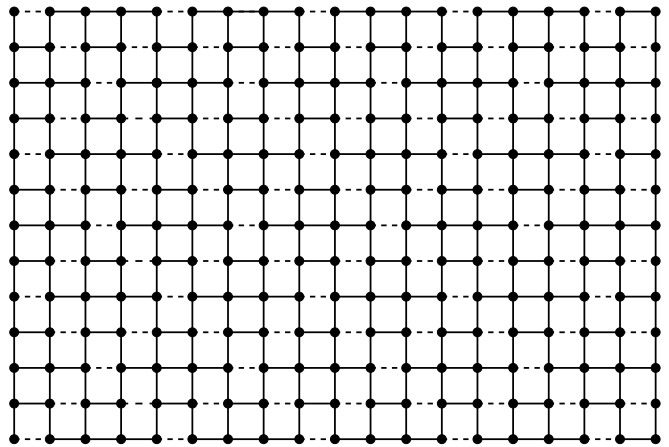


FIG. 6: A patterned lattice in which 50% of elementary square loops are frustrated

In Fig. 7 we divide all qubits into four sets. “Deleted” qubits are represented by empty circles; the severed couplings are represented by dotted lines. “Working” qubits, depicted by large black circles correspond to the nodes of triangular sublattice. Unused “auxiliary” qubits represented by small black circles effectively “pass on” interaction to their neighbors. The “control” qubits represented by gray circles are used to selectively enable or disable antiferromagnetic couplings between working qubits. Deleting gray control qubit switches off an interaction between two working qubits that otherwise are effectively coupled antiferromagnetically. As a next step we apply our construction for embedding a planar graph into a triangular lattice. Note that since for every working qubit we use 2 auxiliary, 3 control qubits and 2 deleted qubits, our estimate for the number of qubits is correspondingly increased by a factor of 8.

For illustrative purposes we give another example shown in Fig. 8. This time a square lattice in which every plaquette is frustrated is mapped onto another square lattice with a lattice constant that is $3\sqrt{2}$ times larger. Now the control qubits can be used not only to switch off the interaction but also to choose its sign. Couplings between a pair neighboring working qubits is controlled

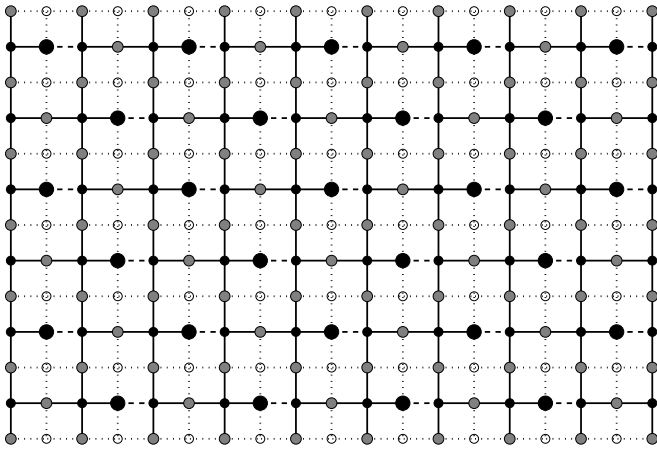


FIG. 7: Mapping onto triangular lattice with antiferromagnetic interactions. Interactions are switched off by polarizing gray qubits.

by two control qubits. Deleting both control vertices severs the interaction between the two working qubits, while deleting only one makes an interaction effectively ferromagnetic or antiferromagnetic, depending on which vertex was deleted.

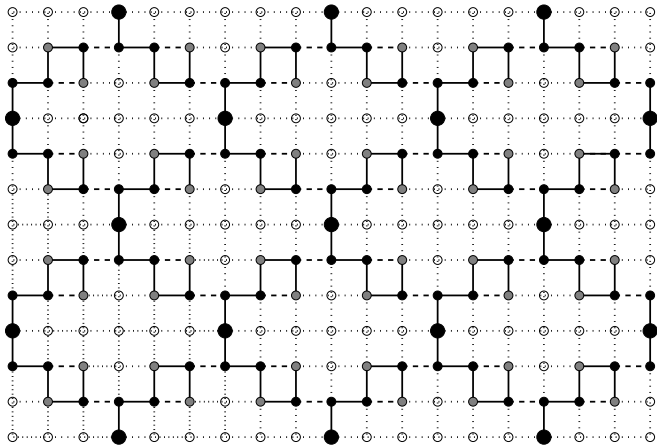


FIG. 8: Mapping onto a square lattice in which nearest neighbor interactions can be made ferromagnetic, antiferromagnetic or can be severed.

Yet another approach is to do graph embedding directly on a lattice. We choose a particular square lattice with frustration where each plaquette has 1 edge of one type (ferromagnetic or antiferromagnetic) and 3 edges of another type. As before, we construct the embedding interactively. Assuming that we constructed an embedding for a subgraph of the original graph so that all eligible vertices lie on the side of the square, we couple the new vertex antiferromagnetically to some of these eligible vertices. This can always be done since we are free to reroute the connections at will. An example is shown in Fig. 9. Control qubits as before are represented by gray circles. For left and right edges we delete either gray qubit. For

the center edge we either delete qubit 2 or both qubits 1 and 3. A simple counting argument shows that since there is a total of 8 choices for control qubits, exactly one will correspond to all couplings being effectively antiferromagnetic. This procedure increases the side of the square by 6 in the worst case, taking the total number of qubits necessary to $36N^2$ in the worst case. As before we stress that this is the worst-case scenario and the estimate will be lowered if better layout algorithms are used.

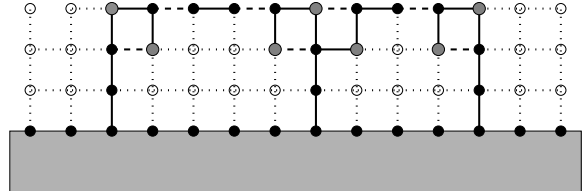


FIG. 9: In the center, either top gray qubit or two bottom gray qubits are deleted. On the sides either of two gray qubits is deleted. Since each elementary square is frustrated it is always possible to make all links antiferromagnetic. A gray area represents a part of the graph that is already embedded.

V. FAULT-TOLERANT COMPUTING

For nanoscale computing architectures it is important to take into account irregularities of the crystal lattice. For classical processing units in molecular computing the following solution was proposed [30]. A massively parallel array of simple computational devices is used, but in contrast to standard architectures, interconnects between devices are redundant (note that both devices and interconnects can be defective). The presence of redundant connections allows to reroute the system once defective elements are identified. Perfectly working system was implemented despite the fact that 10% of elements were defective.

The present AQC architecture, in which individual qubits are “deleted” by polarizing them is perfectly suited to address the problem of fault-tolerant computation. In our model only a small subset of nearest-neighbor couplings are utilized. From this standpoint, the system has large redundancy of links. A computer program, given database of defects, can achieve routings that bypass defects altogether.

This can be easily illustrated as follows. Assume for simplicity that only the following defects can occur: (i) a particular nearest-neighbor coupling is too small in absolute value, $|J_{i,k}| < J$ for some threshold J (see Eq. (5) and discussion after it); (ii) a particular nearest-neighbor coupling has a wrong sign, ferromagnetic when it should be antiferromagnetic or *vice versa*. In either of those cases we mark one of the qubits as “defective”, delete it and route all links around it as shown in the Fig. 10.

Similarly, we can route around qubits that are themselves defective. This can be done as long as individual defects are isolated and their concentration is not too big. In general, it should be possible to reroute around the defects as long as their concentration does not exceed the percolation threshold.

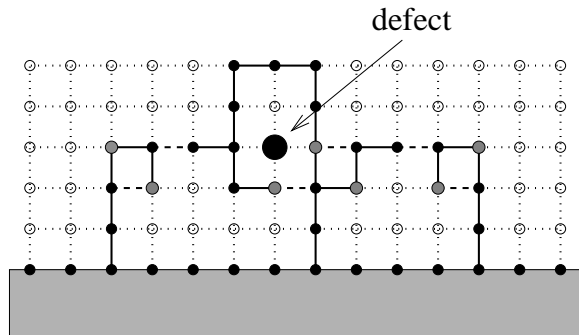


FIG. 10: If it is always possible to route the links around single defect as shown in this figure. A gray area represents a part of the graph that is already embedded.

Moreover, it is possible to do the routing algorithm even when dealing with an entirely random pattern. The number of possible routings increases exponentially with their length and with high probability we can always find at least one routing that makes couplings effectively antiferromagnetic. We expect that this can be done with the number of qubits that differs only by a constant factor compared to the case of regular pattern.

VI. IMPLEMENTATION

There exists a number of requirements for the implementations of the above AQC architecture for solving NP-complete problems. Firstly, the underlying spin lattice must have frustration. Secondly, an interaction between spins must be of the Ising type, $\propto \hat{s}_i^z \hat{s}_j^z$. Thirdly, in our analysis above we assumed only a nearest-neighbor Ising coupling. The above requirements can be satisfied for qubits coupled via the Heisenberg exchange interaction, superconducting qubits, and, except for the last condition, in many systems with “always on” magnetic-dipole and electric-dipole interqubit coupling.

To see this we consider the Hamiltonian \mathcal{H}_{12} for magnetic coupling between the two spins-1/2 located in the plane xy and subject each to a strong static magnetic field $\hat{z} B_\alpha^z$ ($\alpha = 1, 2$). Also each spin is resonantly driven by a weak ac magnetic field $\vec{B}_\alpha^{\text{ac}}(t) = \hat{x} B_\alpha^x \cos(\Omega_\alpha t)$ applied in the orthogonal direction. Assuming that the difference between the values of the Zeeman splitting for the two spins is much greater than their magnetic coupling

we obtain in the rotating wave approximation [24, 32]

$$\mathcal{H}_{12} = - \sum_{\alpha=1}^2 (h_\alpha \hat{\sigma}_\alpha^z + \Gamma \hat{\sigma}_\alpha^x) + [D_{12}(d) + J(d)] \hat{\sigma}_1^z \hat{\sigma}_2^z, \quad (15)$$

$$h_\alpha = \frac{1}{2} (\hbar \Omega_\alpha - \gamma_\alpha B_\alpha^z), \quad \Gamma = -\frac{1}{2} \gamma_\alpha B_\alpha^x,$$

$$D_{12}(d) = \frac{\hbar \gamma_1 \gamma_2}{4d^3}, \quad J(d) \propto \exp(-d/a^*),$$

where

$$|h_j|, |\Gamma_j| \ll \Omega_j, \quad |D_{12}(d)|, |J(d)| \ll \hbar |\Omega_1 - \Omega_2|. \quad (16)$$

In (15) we neglected small terms proportional to \hat{s}_\pm^j which amount to corrections quadratic in $D_{12}/\hbar(\Omega_1 - \Omega_2)$ and $J/\hbar(\Omega_1 - \Omega_2)$. The coefficients $D_{12}(d)$ and $J(d)$ are magnetic-dipole and Heisenberg exchange constants, respectively. Both of them are positive and correspond to antiferromagnetic interaction between spins. Therefore if spins are located at the vertices of a triangular lattice the latter will be frustrated.

By adjusting the amplitudes of the resonant driving fields B_j^x one can set the effective transverse field $\Gamma_j = \Gamma$ for all spins except for the “deleted” spins where there is no ac driving ($\Gamma_j = 0$). Also each ac field $\vec{B}_j^{\text{ac}}(t)$ is not a sequence of short pulses but rather a continuous wave. During the AQC the field detuning from resonance h_j is fixed while the field matrix element $\Gamma = \Gamma(t)$ is decreased adiabatically slow in time. This can be achieved using various methods for a single spin qubit control, such as modification of the electron g-factor [33], and others that are discussed in the context of the spin-based QC in quantum dots [25, 31, 34] and shallow donors [24].

Consider now a triangular lattice of charge qubits where each qubit α is encoded by the two orbital states with the wave functions $\Psi_n^\alpha(x, y, z)$ ($n = 0, 1$) and the difference between the energy levels equals ΔE_j . We assume that the only nonzero dipole matrix elements for each qubit correspond to a z-component of the electric dipole vector, $p_{nm}^j = -e \langle \Psi_n^j | z | \Psi_m^j \rangle$. Consider now a pair of qubits 1 and 2 located in xy plane on a distance d from each other and assume that the strength of the electro-dipole interaction between them $D_{12}(d) \ll \Delta E_1 - \Delta E_2$. Then the truncated 2-qubit interaction Hamiltonian has the form $\mathcal{H}_{12} = D_{12}(d) \hat{s}_1^z \hat{s}_2^z$, where \hat{s}_j^z are z-components of effective spin-1/2 operators acting on qubit states and $D_{12}(d) = (p_{00} - p_{11})^2 / (2 \hbar d^3) > 0$ is a constant of an electro-dipole interaction (cf. [17]). This interaction is of an “antiferromagnetic” type and will lead to frustration on a triangular lattice of qubits located in xy plane.

In a usual QC setting we assume that a control electrode is located near each qubit and apply a time-modulation of the potential of the local electrodes that produces weak microwave fields with the frequencies $\Omega_j \gg |\Omega_j - \Delta E_j|/\hbar$. The z-component of each field will drive resonantly the transition between the corresponding qubit states in a near-field regime. Then in the

rotating wave approximation \mathcal{H}_{12} will take a form (15) ($J = 0$) with h_j and Γ being, respectively, a detuning from the resonance and a non-diagonal matrix element of the field for a qubit j . By fixing $\{h_j\}$ and slowly reducing the value of Γ to zero one can implement the AQC architecture similarly to the previous case. The example given above is relevant for the charge qubits encoded by electron states lithographically confined on a surface of liquid helium [17], and also by laterally quantized electron states in single-electron quantum wells in GaAs heterostructures [19, 21].

A main limitation of the proposed architecture for systems with dipole-dipole interactions is that it takes into account only nearest-neighbor interqubit couplings. We note however that in our approach each vertex of the graph in MIS problem is embedded in a cluster with a large number of qubits. This picture may effectively support the nearest-neighbor coupling approximation. The detailed analysis of this problem will be done elsewhere.

Another challenge of the implementation schemes considered above is that frequencies of resonant driving Ω_j must be different for different qubits and therefore each qubit has to be driven with its own ac field (in near-field regime). For frequency range $\lesssim 10^{12}$ Hz this can be done by modulating the gate bias near each qubit. This condition can be satisfied for electrons on helium [17], for electronic states in broad quantum dots [21] and for spin qubit control via the g-factor modulation [33, 34].

However for qubits encoded by orbital states of a shallow donors in GaAs [35] with the long decay time (~ 350 ns) the intra-qubit frequencies $\Delta E_j/\hbar$ are in the THz range and local ac driving is highly problematic. One could consider in this case a global driving with the THz field containing a range of frequencies within the spectral window that overlaps with the intra-qubits frequencies $\{\Delta E_j/\hbar\}$ so that each qubit will be driven resonantly by its own frequency component of the field. Fixed detuning h_j can be produced locally for each qubit using a quadratic Stark effect from the field of the control electrode.

VII. CONCLUSION AND OUTLOOK OF FUTURE WORK

In the proposed AQC architecture the interactions between qubits are never turned off and never re-adjusted for solving any given instance of an NP-complete problem. Moreover, the problem instances can be embedded into the underlying Ising lattice even in the presence of site imperfections and random distribution of the magnitudes of the Ising coupling coefficients. Also in the proposed scheme there is no need to perform NMR-type refocusing sequences of fast qubit gates that are used in conventional quantum computing (QC) architectures [24, 36] and must satisfy the stringent conditions reflecting the multiple time scales in the material system. In contrary, in our approach the computation pro-

cess is guided with the slow continuous-time variation of the parameters of single-qubit Hamiltonians avoiding unwanted resonances with bulk excitations. These considerations make our analog scalable AQC architecture especially advantageous for solid state QC implementations that use “always on” magnetic- [23, 24, 25] and electric-dipole [17, 18, 19, 20, 21, 22] interactions for entanglement generation. This architecture is also of interest for QC implementations that use the Heisenberg exchange interaction, such as electron spin qubits in quantum dots [25, 31]. It will allow to avoid an inter-qubit “J” gate, or any electrical control over the wavefunction overlap, hence making a gate lithography much simpler and reducing the sensitivity to electrode noise.

For future work we leave the mapping of an instance of the Maximum Independent Set problem onto an arbitrary planar graph, edges of which represent the couplings between qubits. It would allow us to work with completely random systems that do not have any periodic structure. Though the problem of deciding whether a certain instance can be mapped onto an arbitrary planar graph is likely NP-complete, we only need to find a good approximation algorithm, which can be designed to take polynomial time and guarantee to find such a mapping for sufficiently large random planar graph with high probability.

We chose to implement a Maximum Independent Set problem because the problem uniquely permits fluctuations in the magnitude of $J_{i,k}$, as long as the sign is unchanged. For practical problems involving the solution of Constraint Satisfaction problem the problem is often first transformed into an instance of a Maximum Independent Set. Although a mapping from Constraint Satisfaction to Maximum Independent Set exists, it may be beneficial to work with a Constraint Satisfaction problem from the outset. We have described earlier that every clause that involves three variables can be replaced by the gadget in the form of planar graph. Mapping this directly onto Ising model will reduce the number of extra vertices and edges necessary. Maximum Independent Set problem limits our possibilities as it assigns equal weight to every vertex that appears in the independent set. Relaxing this constraint leads for more efficient architectures for simulating a clause or for a gadget that replaces crossing edges.

Recently Oliveira and Terhal developed a mapping of an *arbitrary* quantum circuit onto a square lattice with nearest neighbor interactions of three possible types: $\hat{s}_1^x \hat{s}_2^x$, $\hat{s}_1^y \hat{s}_2^y$, $\hat{s}_1^z \hat{s}_2^z$, or no coupling at all [37]. This opens door for emulating an arbitrary quantum computing algorithm as AQC with all spins on a 2D square lattice.

The construction done in [37] is rigid: every quantum circuit corresponds to a particular lattice. It is interesting to explore if our approach of polarizing qubits to “carve out” circuits out of standard pattern can be applied in the case where couplings $\hat{s}_1^x \hat{s}_2^x$ and $\hat{s}_1^y \hat{s}_2^y$ appear alongside $\hat{s}_1^z \hat{s}_2^z$, and to find out what might be the optimal standard pattern. In addition it is interesting to explore if the same

can be accomplished starting off from a completely random pattern. If a standard pattern is sufficient (provided we can adjust fields acting on individual qubits), it may be a very practical approach for solid-state implementations of a universal quantum computer and could be programmed to implement Shor's factoring algorithm.

VIII. ACKNOWLEDGMENTS

We gratefully acknowledge M.I. Dykman (Michigan State University) for stimulating discussions. This

work was supported by the National Security Agency (NSA) and Advanced Research and Development Activity (ARDA) under Army Research Office (ARO) contract number ARDA-QC-P004-J132-Y05/LPS-FY2005.

-
- [1] M.R. Garey and D.S. Johnson, *Computers and Intractability. A Guide to the Theory of NP-Completeness* (W.H. Freeman, New York, 1997)
- [2] M. Mezard, G. Parizi, and M. Virasoro, *Spin glass theory and beyond* (World Scientific, Singapore, 1987).
- [3] E. Farhi, et al., arXiv:quant-ph/0001106.
- [4] E. Farhi, J. Goldstone, S. Gutmann, J. Lapan, A. Lundgren, and D. Preda, *Science* **292**, 472 (2001).
- [5] V. N. Smelyanskiy, S. Knysh, and R. D. Morris Phys. Rev. E **70**, 036702 (2004)
- [6] J. Brooke, et al, *Science*, v. 284, p. 779 (1999).
- [7] F. Barahona, J. Phys. A: Math. Gen. **15** 3241 (1982).
- [8] G. E. Santoro, et al, *Science*, v. 295, p. 2447 (2002).
- [9] R. Giraud, et al., Phys. Rev. Lett **87**, 057203 (2001).
- [10] (a) S. Ghost, et al., *Science* **296**, 2195 (2002); (b) S. Ghost, et al., *Nature* **425**, 48 (2002).
- [11] P.C.E. Stamp and I.S. Tupistyn, Phys. Rev. B **69**, 014401 (2004).
- [12] Y. Makhlin, G. Schön, and A. Shnirman, Rev. Mod. Phys. **73** 357 (2001).
- [13] J.E. Mooij, et al., *Science* **285** 1036 (1999).
- [14] Yu. A. Pashkin, et al., *Nature* **421**, 823 (2003).
- [15] A.J. Berkley, et al., *Science* **300**, 1548 (2003).
- [16] M.H. Devoret, A. Wallraff and J.M. Martinis, cond-mat/0411174.
- [17] (a) P.M. Platzman and M.I. Dykman, *Science* **284** 1967 (1999); (b) M.I. Dykman M I and P.M. Platzman, *Fortschr.* **48**, 1095 (2000).
- [18] L. Fedichkin, M. Yanchenko and K.A. Valiev, *Nanotechnology* **11**, 387 (2000); L. Fedichkin and A. Fedorov Phys. Rev. A **69**, 032311 (2004).
- [19] W.G. Van der Wiel W G, et al., Rev. Mod. Phys. **75**, 1 (2003).
- [20] L. C. L. Hollenberg, et al., Phys. Rev. B **69**, 113301 (2004).
- [21] B. Golding, M.I. Dykman, cond-mat/0309147.
- [22] V. N. Smelyanskiy, A. G. Petukhov, V. V. Osipov, Phys. Rev. B **72**, 081304 (2005); see also quant-ph/0407220.
- [23] J. Tejada, et al, *Nanotechnology* **12**, 181 (2001).
- [24] R. de Sousa, J. D. Delgado, and S. Das Sarma Phys. Rev. A **70**, 052304 (2004).
- [25] V. Cerletti, et al, arXiv:cond-mat/0412028.
- [26] W. M. Kaminsky, S. Lloyd, T. P. Orlando, "Scalable Architecture for Adiabatic Quantum Computing of NP-Hard Problems", in *Quantum Computing & Quantum Bits in Mesoscopic Systems* (Kluwer Academic 2003).
- [27] M. R. Garey, D. S. Johnson, L. Stockmeyer, Proceedings of the sixth annual ACM symposium on Theory of computing, p.47 (1974).
- [28] M.J. Storcz and F.K. Wilhelm, Appl. Phys. Lett. **83**, 2387 (2003).
- [29] Throughout the paper we refer to the coupling between spins as being "effectively" ferromagnetic or antiferromagnetic if the chain of edges of the graph connecting the spins contains even (odd) number of antiferromagnetic links.
- [30] J.R. Heath, P.J. Kuekes, G.S. Snider, R.S. Williams, *Science* **280**, 1717 (1998).
- [31] D. Loss and D.P. DiVincenzo, Phys. Rev. A **57**, 120 (1998).
- [32] C.P. Slichter, *Principles of Magnetic Resonance*, 3rd Ed. (Springer-Verlag, Berlin, 1996).
- [33] G. Salis, et al, *Nature* **414**, 619 (2001).
- [34] D. Loss, G. Burkard and D. P. DiVincenzo, *Journal of Nanoparticle Research* **2**, 401 (2000).
- [35] D.G. Allen, C.R. Stanley and M.S. Sherwin, arXiv:quant-ph/0503056.
- [36] P. Sengupta and L. P. Pryadko Phys. Rev. Lett. **95**, 037202 (2005).
- [37] R. Oliveira, B. Terhal, arXiv:quant-ph/0504050.